

Customize-It-3D: High-Quality 3D Creation from A Single Image Using Subject-Specific Knowledge Prior

Nan Huang
Peking University
hannahuang411@gmail.com

Ting Zhang
Microsoft Research
tinzhan@microsoft.com

Yuhui Yuan
Microsoft Research
yuyua@microsoft.com

Dong Chen
Microsoft Research
doch@microsoft.com

Shanghang Zhang
Peking University
shanghang@pku.edu.cn

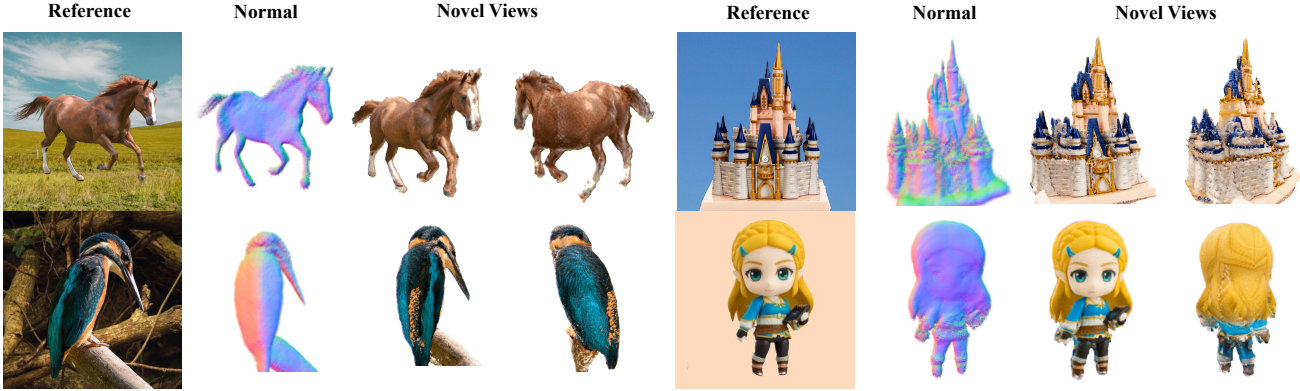


Figure 1. *Customize-It-3D* has the capability to generate high-fidelity 3D content from just a single image. We present the normal map and novel-view renderings for general objects, highlighting the consistency texture and geometry with remarkable quality at novel views.

Abstract

In this paper, we present a novel two-stage approach that fully utilizes the information provided by the reference image to establish a customized knowledge prior for image-to-3D generation. While previous approaches primarily rely on a general diffusion prior, which struggles to yield consistent results with the reference image, we propose a subject-specific and multi-modal diffusion model. This model not only aids NeRF optimization by considering the shading mode for improved geometry but also enhances texture from the coarse results to achieve superior refinement. Both aspects contribute to faithfully aligning the 3D content with the subject. Extensive experiments showcase the superiority of our method, *Customize-It-3D*, outperforming previous works by a substantial margin. It produces faithful 360-degree reconstructions with impressive visual quality, making it well-suited for various applications, including text-to-3D creation. Our project page is:

<https://nnanhuang.github.io/projects/customize-it-3d/>

1. Introduction

3D creation from a single image remains a profoundly intricate challenge, due to its inherently ill-posed nature, arising from the significant information gap between a single 2D image and the comprehensive 3D spatial and textural properties of the depicted object. Despite its great challenge, recent works [38, 46, 58, 60, 69] have achieved notable results in image-to-3D creation. They draw inspiration from text-to-3D methods [45, 65] which utilize score distillation sampling (SDS) loss to optimize a neural radiance field (NeRF). This SDS loss serves as a guiding principle for novel view synthesis, emulating the way humans utilize priors to infer 3D shape and texture from a single image. While these methods tend to produce promising results, they still exhibit noticeable inconsistencies when compared with the reference view, either in context of the geometry (*i.e.*, multi-face

issue) or from the texture perspective (novel views often lack fidelity, presenting smooth and disruptive particulars).

When crafting intricate 3D models of a specific object, a professional artist indeed need not be equipped with an exhaustive understanding of all the objects in the natural world. Rather, the essential requirement lies in possessing specialized, profound knowledge pertaining to that specific subject at hand. This targeted expertise shall be more instrumental in the meticulous creation of 3D assets. Despite incorporating several adjustments such as CLIP loss and textual inversion considered in [46, 60], the supervision of novel views still relies on a general text-to-image model [3, 18, 49, 51, 53], which has challenge in producing consistent results based solely on text, given the inherent difficulty in crafting textual descriptions to encompass every detail. Consequently, these approaches struggle to maintain consistency and fall short in reconstructing high-fidelity 3D objects. This realization has inspired us to explore strategies for cultivating subject-specific knowledge prior, aiming to achieve high-quality image-to-3D creation.

We propose *Customize-It-3D*, a novel approach that fully unleashes the geometry/appearance information provided by the reference image to promote customized knowledge prior for 3D generation. *Customize-It-3D*, like the previous methods mentioned above, adopts a two-stage framework in a coarse-to-fine manner. However, it is guided with subject-specific knowledge prior.

In the first stage, we optimize a neural radiance field to learn an implicit volume representation. The reference view is directly supervised through rendering loss, specifically pixel differences. For novel views, unlike conventional approaches employing general T2I models for SDS loss, we use a subject-specific T2I model. There has been remarkable success in subject-driven image generation [29, 52]. They typically demand at least 3 to 5 images capturing the same subject with varying contexts in order to model the key visual features of the subject. However, our scenario presents a challenge as we possess only a solitary image, which may potentially misguide the model to a trivial solution (mode collapse). To surmount this limitation, we propose to exploit multiple modalities extracted from the reference image, namely depth map, mask image, and normal map. Furthermore, by adjusting the model to be cognizant of the subject’s geometry information, we can supervise NeRF generation in a more fine-grained manner, particularly by taking the shading mode into consideration.

While NeRF is renowned for effectively learning complex geometries, their proficiency in generating intricate texture details is hindered by significant memory demands. Therefore, our objective in the second stage is to enhance visual realism by transforming the coarse NeRF model into point clouds. Conversion to point clouds allows us to have the desirable groundtruth textures on the reference view

through projection. Yet we observe that constructing point clouds from depth images as in [60] tends to introduce geometric inaccuracies since NeRF does not store any 3D geometry explicitly (only the density field). In lieu of this, our novel strategy entails an initial step of mesh generation, followed by the established mesh regularization techniques to refine the shape, before sampling points on the mesh surface. In addition, we harness the potential of the aforementioned subject-specific Text-to-Image (T2I) diffusion model, effectively elevating the texture realism, before extending the RGB rendering from the coarse NeRF to point clouds. This augmentation is shown to yield superior texture quality in the final outcomes.

Besides employing the proposed subject-specific 2D diffusion prior, we also utilize a 3D prior to further guide the training process as in [46], compensating the 3D information. Note that this 3D prior takes the reference image as input and thus both the adopted 2D and 3D prior are subject-specific knowledge priors to guide the novel views. To evaluate our method, we collect a benchmark consisting of 100 images. We compare *Customize-It-3D* with prior state-of-the-arts on RealFusion15 [38], and our Customize100 dataset. Extensive experiments demonstrate our method achieves significant improvement in visual quality in context of accurate geometry and realistic details. In summary, our contributions are:

- We propose *Customize-It-3D*, an innovative framework for the generation of high-quality 3D content from a single image by utilizing a subject-specific diffusion prior, which is designed to enhance the personalization of 3D content creation for specific subjects.
- We introduce a multi-modal DreamBooth model that promotes comprehensive knowledge priors derived from multi-modal images of the subject, prioritizing the faithfulness of the diffusion model to the reference image. This knowledge prior not only facilitates NeRF optimization based on the shading mode but also enhances the texture of the initial coarse results for better refinement.
- The resulting framework demonstrates state-of-the-art performance in 3D reconstruction using a diverse range of in-the-wild images and images from existing datasets. Furthermore, this approach opens up intriguing possibilities, such as text-to-3D content creation.

2. Related work

Multi-view 3D reconstruction. Early works [1, 14, 54, 55] traditionally require a dense set of input images to accurately deduce geometry by establishing correspondence within the overlapping regions.. The advent of NeRF [36, 39] and its variants [5, 6, 41] have significantly propelled the quality of synthesized novel views through the reconstruction of 3D scenes via implicit neural representations. Subsequent efforts [11, 20, 25, 71] have been dedicated to

the facilitation of NeRF optimization from a sparser set of input views. Typically they entail the extraction of per-view features from each input image and aggregate multi-view features for each point along the camera ray. This aggregated information is then decoded to determine density (or Signed Distance Function, SDF) and colors. Diffusion models, which have demonstrated significant advancements in general image synthesis, has emerged as a recent focal point in 3D generation research. Some studies endeavor to directly train 3D diffusion models based on diverse 3D representations, including point clouds [37, 42, 73, 76], meshes [15, 35], neural fields [2, 7, 9, 13, 16, 17, 22, 24, 26, 28, 43, 64, 74]. Others, such as [4, 57, 59, 66] conceptualize 3D generation as an image-to-image translation task and directly generate coherent multiview color images, as exemplified by Zero123 [34]. It’s noteworthy that both approaches require access to multi-view images for training. However, a recurring challenge in this domain lies in the constrained availability of expansive 3D assets datasets. Consequently, most studies have been confined to evaluation on limited categories of shapes or encounter difficulties in extending their models effectively on general objects.

3D generation using knowledge prior. A surge of approaches have been study leveraging large models pre-trained on billions of images as knowledge prior to guide the 3D synthesis, circumventing the need for large-scale 3D datasets. One popular task is text-to-3D synthesis, given the exceptional breakthroughs in text-to-image generation. Pioneering works [40, 56] such as DreamFields [21], DreamFusion [45] and SJC [63] have demonstrated success of incorporating NeRF-like models with frozen generative systems for optimization-based 3D synthesis. They fed the rendered 2D images to diffusion models or CLIP model for calculating losses to guide the 3D shape optimization. It sparked numerous follow-up works improve such per-shape optimization scheme in the context of 3D representations [8, 30, 32, 61], sampling schedules [19], and loss design [65], subject-driven editing [48]. An alternative avenue of research [33, 38, 46, 60] seeks to generate 3D digital content from a single image, offering a more precise and controllable approach than text-based methods. The prevailing majority of existing endeavors in this area remain rooted in optimization-based techniques, achieving this task by imposing pixel-wise reconstruction losses on the reference view, in addition to inheriting the SDS loss from text-to-3D methodologies. In comparison, we also follow the DreamFusion pipeline [45], but with a focus on cultivating subject-specific knowledge prior. While Dreambooth3D [48] also leverages a subject-specific diffusion prior, it requires multiple subject images and is designed for text-to-3D editing. In contrast, our approach tackles a more challenging scenario with only one image and introduces a multi-modal diffusion prior, specifically aiming at image-to-3D generation.

3. Method

Generating a personalized 3D object from a single image is a highly challenging task, because it involves disclosing the identity, geometric shape, and texture from limited and incomplete visual information. Therefore, we propose a two-stage coarse-to-fine framework, *Customize-It-3D*, leveraging carefully cultivated subject-specific knowledge prior to effectively constrain the coherency of 3D object with respect to a particular identity. The proposed framework is illustrated in Figure 2. We will first detail our subject-specific knowledge prior and then introduce our method.

3.1. Subject-Specific Knowledge Prior

Subject-Specific 2D Prior: Multi-modal DreamBooth. Current text-to-image diffusion models possess rich semantic knowledge and 2D image knowledge. DreamFusion [45] is a pioneering work that utilizes the latent knowledge of these diffusion models to guide a 3D representation optimization. However, due to the abundant imagination of 2D diffusion models, it is challenging to precisely control over the generated geometric shapes, textures, and identities using solely text, resulting in discrepancies and thereby causing confusion in guiding 3D reconstructions. This phenomenon tends to produce smoothed textures and imprecise geometries as a result of averaging the inconsistent outcomes. To address this issue, we undertake a fine-tuning process on a pre-trained text-to-image diffusion model using a single reference image. To mitigate the risks of overfitting and mode collapse, we choose to leverage multi-modal images in our approach.

Specifically, we first utilize a pre-trained monocular depth estimator [50] and a single-view normal estimator [12] [23] to obtain the depth and normal maps of the reference image. Furthermore, we segment the last channel of the input image to obtain a mask map. Then, we use this image set and the reference image together to partially fine-tune Stable Diffusion [51] with Dreambooth [52], so that it learns to bind a unique identifier with the specific subject embedded in the output domain of the model. We also find that a fully trained Dreambooth tends to overfit the subject viewpoints in input images, leading not only to a severe Janus problem but also reducing diversity, as noted in previous work [48]. Therefore, we only use the partially fine-tuned results. Unlike Dreambooth [52], we fine-tune not only the UNet but also the text encoder, which leads to better results.

Additionally, we utilize a prior preservation loss, which enables the supervision of model training during fine-tuning with self-generated images x_{ori} from the original diffusion model. Then our loss function to finetune a diffusion model

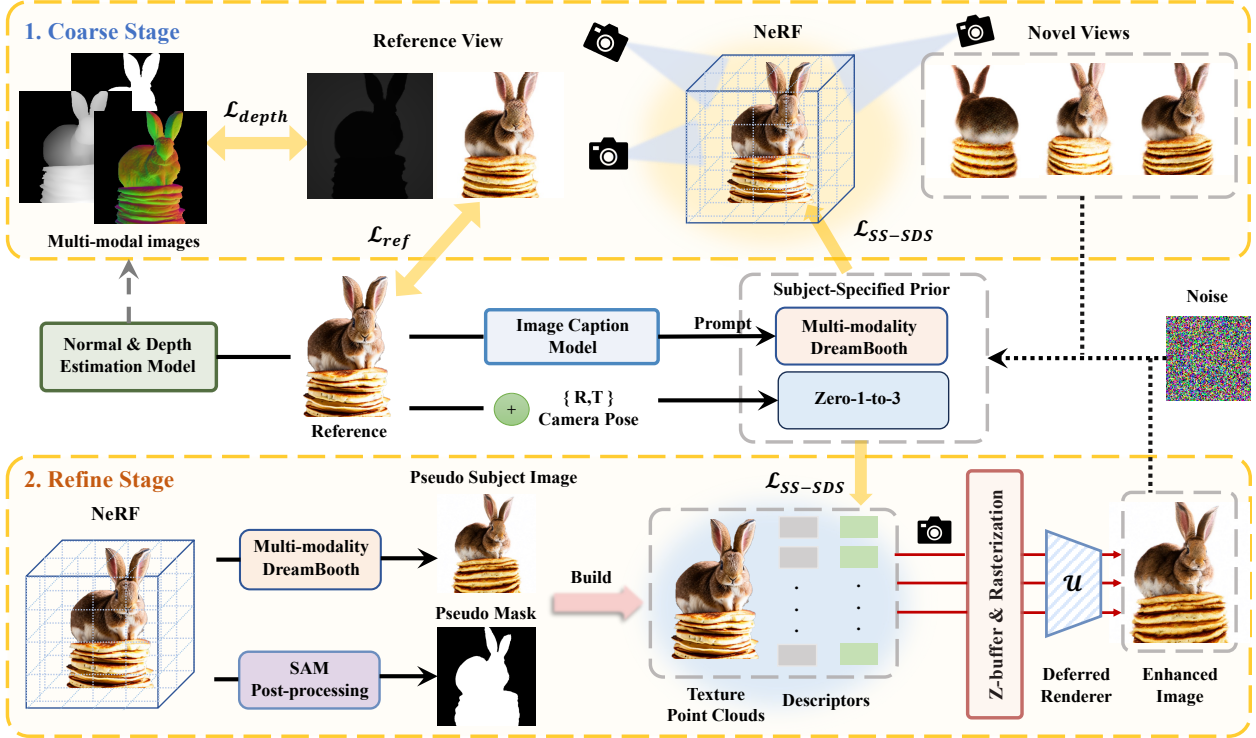


Figure 2. We propose a two-stage framework for high-quality 3D creation from a reference image with subject-specific diffusion prior (Sec. 3.1). At the coarse stage, we optimize a NeRF for reconstructing the geometry of the reference image in a shading-aware manner (Sec. 3.2). We further build point clouds with enhanced texture from the coarse stage, and jointly optimize the texture of invisible points and a learnable deferred renderer to generate realistic and view-consistent textures (Sec. 3.3).

ϵ_ϕ is :

$$\mathbb{E}_{x,c,\epsilon,\epsilon',t}[w_t \|\epsilon_\phi(\alpha_t \mathbf{x} + \sigma_t \epsilon, c) - \mathbf{x}\|_2^2 + \lambda w_{t'} \|\epsilon_\phi(\alpha_{t'} \mathbf{x}_{ori} + \sigma_{t'} \epsilon', c_{ori}) - \mathbf{x}_{ori}\|_2^2], \quad (1)$$

where \mathbf{x} is the reference image and α_t, σ_t, w_t control the noise schedule, c_{ori} is the prompt to generate x_{ori} . The second term is prior-preservation loss with weight λ .

In terms of prompt processing, we need an identifier with a weak prior in both the language model and the diffusion model. Therefore, we follow previous work [62] and use the “sks” identifier for stable diffusion [51]. Differently, since we are dealing with a set of images with different modalities, it is imperative not to employ an identical prompt for all images, as this practice can introduce confusion to the model and lead it to erroneously emphasize common distinctive features. Our primary objective is not to model the shared aspects across all modalities but rather to equip the model with the capability to discern and accommodate the distinctions arising from different modalities. Thus, we incorporate additional instructions, and the prompt c for fine-tuning the diffusion model takes the form of “a depth map / normal map / foreground mask / rgb photo of sks [class name]”. The choice of the specific instruction is made in accordance with the given modality during training. In this

way, the model is encouraged to perceive the subject from different perspectives, enriching its subject-specific prior.

Subject-Specific 3D Prior: Viewpoint and Image-Conditioned Diffusion Model. Presently, large-scale pre-trained diffusion models are primarily trained on 2D images, lacking substantial 3D-specific knowledge. Notably, the recent Zero-1-to-3 model [34] stands out as it utilizes fine-tuning on a synthetic 3D dataset [10] to develop a viewpoint-conditioned diffusion model. This model takes a reference image along with related external camera parameters as inputs, enabling the generation of novel views of the same subject based on the reference image. Therefore, it serves as our preferred strategy for establishing a subject-specific 3D prior, contributing to improving 3D consistency.

3.2. Coarse Stage: Image to 3D Reconstruction

In the coarse stage, we aim to obtain the approximate geometric structure of the 3D object and the rough texture necessary for constructing a textured point cloud. In this stage, our scene model is a neural field based [39] on Instant-NGP [41]. This choice is made because it can handle complex topological changes in a smooth and continuous manner while also enabling the reconstruction of 3D objects in a relatively fast and computationally efficient manner.

Subject-specific knowledge prior for novel views. We

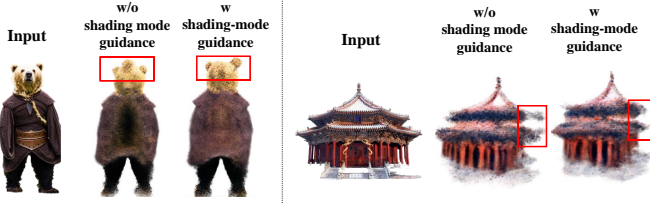


Figure 3. The proposed shading mode-aware guidance largely enhances the 3D geometry in the coarse stage.

optimize the neural radiance field such that its multi-view renderings look like high-quality samples using the subject-specific diffusion model. Specifically, let the rendered image $\mathbf{I} = \mathcal{G}_\theta(\mathbf{v})$ at the viewpoint \mathbf{v} , where \mathcal{G} is the differentiable rendering function for NeRF optimization parameterized by θ . We employ the multi-modal DreamBooth model as a 2D prior and follow [45] [32] to use the score distillation (SDS) loss, which assigns a “score” to the rendered image, guiding the optimization of the 3D model’s parameters θ towards the direction of higher density regions.

Differently, we go beyond this and propose modifying the text prompt based on the specific NeRF shading mode. This modification is aimed at fully harnessing the capabilities of our multi-modal diffusion model to offer precise guidance tailored to different NeRF shading modes, which is facilitated by the inherent multi-modal awareness of our finetuned diffusion model. To elaborate, given the text prompt y that is generated from an image captioning model [31] from the reference image, we adapt the text prompt to “sks normal map of y ” when the NeRF rendering employs “normal” shading mode and “sks rgb photo of y ” when the NeRF rendering utilizes “albedo” shading mode. By enforcing consistency between the rendered image aligned with the modified text prompt, the multi-modal diffusion model is able to provide more accurate guidance and thus enhance the quality of the 3D reconstruction, as illustrated in Figure 3. Formally, we use 2D SDS loss as:

$$\nabla_\theta \mathcal{L}_{SS2D} = \mathbb{E}_{t,\epsilon} [w(t)(\epsilon_\phi(\mathbf{z}_t; y_m, t) - \epsilon) \frac{\partial \mathbf{z}}{\partial \mathbf{I}_m} \frac{\partial \mathbf{I}_m}{\partial \theta}], \quad (2)$$

where $\mathbf{I}_m = \mathcal{G}_\theta(\mathbf{v}, m)$ and m denotes the shading mode and can take on values of either “normal” or “albedo”. We use the personalized text prompt y_m to encode NeRF’s novel view rendering \mathbf{I}_m to the noisy latent \mathbf{z}_t by adding a random Gaussian noise ϵ of a timestep t .

In addition, we have the subject-specific 3D prior for novel view guidance, which can be formulated as follows:

$$\mathcal{L}_{SS3D} = \mathbb{E}_{t,\epsilon} \left[w(t)(\epsilon_\phi(\mathbf{z}_t; \mathbf{x}, t, R, T) - \epsilon) \frac{\partial \mathbf{I}}{\partial \theta} \right], \quad (3)$$

where R, T represent the camera’s rotation and translation, and \mathbf{x} stands for the input reference image. Here, we do not utilize text as guidance but instead use image-based guid-

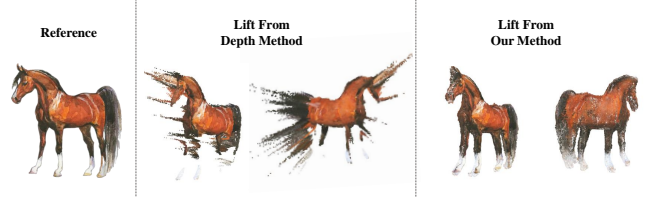


Figure 4. Illustrating different point cloud building methods from (1) depth images as in [60] and (2) our method.

ance, specifically the relative camera transformations between viewpoints.

The overall supervision is:

$$\nabla_\theta \mathcal{L}_{SS-SDS} = \lambda_{SS2D} \nabla_\theta \mathcal{L}_{SS2D} + \lambda_{SS3D} \nabla_\theta \mathcal{L}_{SS3D}, \quad (4)$$

where λ_{SS2D} and λ_{SS3D} are their weights respectively.

Groundtruth knowledge for the reference view. Under the reference view \mathbf{v}_{ref} , the rendered image $\mathbf{I} = \mathcal{G}_\theta(\mathbf{v}_{ref})$ by NeRF should be consistent with the input image \mathbf{x} to align with our goal of customizing 3D objects. Therefore, we utilize the pixel-wise difference between the NeRF rendering and the input image under the reference view as one of our major losses:

$$\mathcal{L}_{ref} = \|\mathbf{x} \odot M - \mathcal{G}_\theta(\mathbf{v}_{ref})\|_1, \quad (5)$$

where \odot is Hadamard product. And we follow previous work [70] to apply foreground mask M in order to get extracted object which will ease the geometry reconstruction.

Using only the RGB per-pixel losses can lead to poor quality geometry issues such as sunken faces, overflattening, due to the inherent shape ambiguity in 3D reconstruction. To mitigate this issue, we employ MiDaS [50], a pretrained monocular depth estimator, to estimate the depth d_{ref} of the reference image. However, since the estimated pseudo depth may not be accurate and there is a scale and source mismatch with the depth d from NeRF, we regularize the negative Pearson correlation between the pseudo depth and the depth from NeRF under the reference viewpoint,

$$\mathcal{L}_{depth} = -\frac{\text{Cov}(d_{ref}, d)}{\text{Var}(d_{ref})\text{Var}(d)}. \quad (6)$$

Here $\text{Cov}(\cdot)$ denotes covariance and $\text{Var}(\cdot)$ measures standard deviation. We employ this function as our depth regularization to encourage the NeRF output d under the reference view to be close to the depth prior.

Overall training. In summary, the loss in the coarse stage consists of the following parts: \mathcal{L}_{ref} , \mathcal{L}_{SS-SDS} and \mathcal{L}_{depth} . During training, we follow [60], adopting a progressive training strategy. We start by training only in a partial region of the object’s front view, and then gradually expand the training scope.

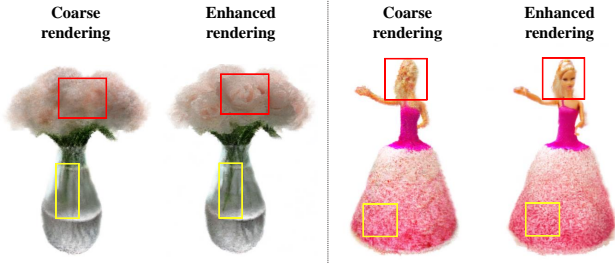


Figure 5. The texture details from coarse rendering are largely enhanced using the multi-modal DreamBooth.

3.3. Refine Stage: Neural Texture Enhancement

In the coarse stage, due to the computationally intensive nature of NeRF optimization, we only perform optimization at low resolutions. Moreover, due to the inherent limitations of NeRF, such as the tendency to produce high-frequency artifacts [45], we can only obtain a low-resolution, low-texture-quality 3D model. As a result, we are motivated to explore alternative representations for NeRF, particularly focusing on transforming it into an explicit point cloud. Point clouds have the advantage of allowing direct projection of images, preserving high-quality frontal texture details, and offering opportunities for personalization and enhancement of the projected images, fulfilling the needs of high-quality customized 3D models. In summary, our goal in the refine stage is to retain the geometric structure of the coarse stage, generate a dense point cloud, and optimize the textures not visible in the reference view \mathbf{v}_{ref} , as we directly project the frontal reference image \mathbf{x} onto the point cloud. We elaborate several key designs to facilitate the transformation from the coarse to the refine stage.

Point cloud building. Past work has focused on constructing a point cloud from multi-view RGBD images under NeRF rendering [60]. However, due to noise in RGBD images and inaccurate depth estimation, the generated point cloud is very noisy and inaccurate, significantly impairing the 3D geometry in refine stage. To address this, we export the NeRF in coarse stage as a mesh, utilizing mesh regularizations and perform Poisson sampling on the mesh to obtain a dense point cloud P^m . Figure 4 shows this difference. We opt to a point cloud because it allows personalized diffusion model-based texture enhancement for each viewpoint, resulting in a higher-quality point cloud that better aligns with our customized 3D object generation needs.

Texture projection. However, since NeRF-rendered images from different viewpoints may have overlapping regions, a 3D point may be assigned different colors under different viewpoints [67], leading to texture conflicts. Therefore, we propose an iterative strategy for constructing a clean texture point cloud P from mesh sampled point cloud P^m . Initially, we trust all points P_{ref}^m under reference view \mathbf{v}_{ref} and use a reference mask M to perform

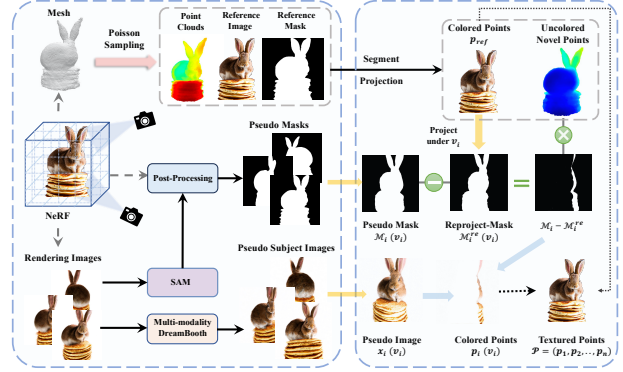


Figure 6. Illustrating the textured point cloud construction. We enhance the texture and mask of novel views and iteratively project texture to the point cloud.

color mapping on P_{ref}^m , obtaining the front-facing perspective of the new point cloud P_{ref} . For novel view projection, we aim to avoid introducing points that overlap with P_{ref} . Hence, we proceed to project the recently obtained point cloud P_{ref} onto each novel view \mathbf{v}_i to generate a new mask denoted as $M_{\mathbf{v}_i}^{ref-proj}$. We then project textures to the points under this novel view only when these points belong to the set difference between the novel view mask $M_{\mathbf{v}_i}$ and the reprojected mask $M_{\mathbf{v}_i}^{ref-proj}$. Finally we have a clean point cloud $P = \{P_{ref}, P_1, \dots, P_n\}$ which ensures color mapping is done without introducing conflicts.

Texture and mask enhancement. The texture quality obtained in the coarse stage is suboptimal. Therefore, prior to projecting the reference image \mathbf{x} from the reference view and rendered RGB images $\mathcal{X} = \{\mathbf{x}_{\mathbf{v}_1}, \mathbf{x}_{\mathbf{v}_2}, \dots, \mathbf{x}_{\mathbf{v}_n}\}$ under novel views onto the point cloud geometry, we perform a texture enhancement process on all rendered images within \mathcal{X} . Specifically, we add noise to the rendered images and leverage the previously fine-tuned multi-modal personalized diffusion model to denoise into a set of pseudo images \mathcal{X}^{pseudo} that possess higher texture quality as well as multi-view consistency. Figure 5 shows that the texture details can be significantly improved by utilizing our multi-modal DreamBooth model.

Simultaneously, due to the issues in the coarse stage of NeRF, the generated masks $\mathcal{M} = \{M_{\mathbf{v}_1}, M_{\mathbf{v}_2}, \dots, M_{\mathbf{v}_n}\}$ by NeRF are not satisfactory. Fine details (for example long and thin parts) in the object structure may be compromised, leading to defects in point cloud texture and geometry initialization due to mask inadequacies. Therefore, we adopt Segment Anything Model (SAM) to generate more refined and accurate masks \mathcal{M}^{pseudo} . However, due to the insufficient resolution of RGB images and the noise introduced by SAM, we assess the quality of the generated mask by relying on SAM’s score. Only when the quality surpasses a certain threshold do we consider using this mask; otherwise, we adhere to utilizing masks generated by NeRF.

	LPIPS↓	PSNR↑	CLIP↑
RealFusion [38]	0.193	16.87	73.50%
Make-It-3D [60]	0.119	20.01	83.90%
Magic123 [46]	0.100	19.50	82.00%
Customize-It-3D (Ours)	0.094	20.50	90.90%

Table 1. Quantitative comparison on RealFusion15. We compute LPIPS and PSNR under the reference view, and CLIP under novel views.

We illustrate our textured point cloud building in Figure 6.

Deferred point cloud rendering and training. After initializing the geometry and texture of the point cloud P , a focus is placed on enhancing the texture of the point cloud in novel views with subject-specific prior. Specifically, we assign a 19-dimensional descriptor F to each point in the novel view \mathbf{v} , where the first three dimensions are colors initialized from the above process. During the rendering of the point cloud, we employ a deferred rendering scheme [60], rendering the point cloud K times at different resolutions and concatenating the resulting K feature maps into the final image using a jointly optimized U-Net network denoted as \mathcal{R}_θ . The refine stage’s loss is similar to that in Sec. 3.2, with the addition of a regularization term penalizing excessive differences in texture between the refined and initialized states.

4. Experiments

4.1. Implementation Details

Optimizing the pipeline. For the supervision of Subject-Specific Knowledge Prior, we set the weights of λ_{2D} and λ_{3D} to 1 and 40, akin to the approach in [46]. Additionally, the weight of λ_{3D} is adjusted based on the relative distance from the frontal view. We utilized the fine-tuned multi-modal DreamBooth and Zero123 as 2D and 3D priors, with guidance scale set to 10 and 5 [34], respectively. Additionally, we randomly sampled t from 200 to 600 and employed classifier-free guidance to compute the SDS loss. **NeRF and point cloud rendering.** We employ multi-scale hash encoding from Instant-NGP [41] and maintain an occupancy grid to skip empty space for improving rendering efficiency. Additionally, we incorporate shading augmentations, such as Lambertian shading similar to [45]. However, during the first 1000 iterations of the second phase of progressive training, we utilize normal shading to emphasize the learning of better geometry. For the deferred rendering strategy of point clouds, we utilize a 2D U-Net architecture with gated convolutions [72].

4.2. Comparisons with the State of the Arts

Baselines. We compare our approach against recent state-of-the-art methods: RealFusion [38], Make-It-3D [60], and Magic123 [46] (using Zero123 XL checkpoint [34] as ours

for fair comparison). We compare these methods using the RealFusion dataset [38] and a customized dataset we created. The RealFusion dataset includes many natural images, while our customized dataset comprises real images and images generated by Stable Diffusion XL [44]. We evaluate all the baseline methods using their official code.

Qualitative comparison. We present a comprehensive collection of qualitative results in Figure 7. RealFusion often generates flat 3D results with colors and shapes that diverge significantly from the input image. Make-it-3D exhibits competitive texture quality but suffers from an issue known as long geometry in side views, particularly noticeable in the reconstruction of objects such as chairs. Magic123 produces visually plausible structures but grapples with a notable issue of multi-face, as it tends to replicate the reference texture in the back view. In contrast, our approach can reasonably hallucinate the texture details and geometry for novel views that even deviate significantly from the reference image, which greatly improves the fidelity and consistency in creating 3D models.

Quantitative comparison. We quantitatively compare with the baselines in Table 1. We use metrics following [46, 60] with PSNR, LPIPS [75], and CLIP-similarity [47]. As shown in the table, Customize-It-3D achieves Top-1 performance across all the metrics, showing that our model is able to generate 3D objects with better 3D consistency.

5. Ablations and Analysis

With or without multi-modal DreamBooth. We first ablate the effect of using the proposed multi-modal DreamBooth in Figure 8. We observe a consistent improvement in terms of both texture and geometry. Employing the suggested multi-modal subject-specific diffusion model prior results in higher-quality 3D content, yielding more compelling visuals with enhanced 3D consistency.

Single RGB versus multi-modal. We experiment a baseline that employs conventional DreamBooth finetuned from a single RGB reference to further investigate the impact of our shading mode-aware multi-modal guidance. The difference shown in Figure 9 demonstrate a clear improvement, whereas the baseline suffers from multi-face problem.

6. Applications

High-quality text-to-3D generation. To achieve high-quality text-to-3D creation, we initially utilize a T2I diffusion model to convert the text prompt into a reference image and then pass it into our image-based 3D creation method. We show the results in Figure 10. Customize-It-3D demonstrates remarkable quality in text-to-3D generation.

Real scene modeling. We extend our model evaluation to real-world scenarios by inputting arbitrary general images capturing complex, authentic scenes into our framework.



Figure 7. Qualitative comparison on image-to-3D generation. We compare Customize-It-3D to RealFusion [38], Make-it-3D [60] and Magic123 [46] for creating 3D objects from a single unposed image (the leftmost column).

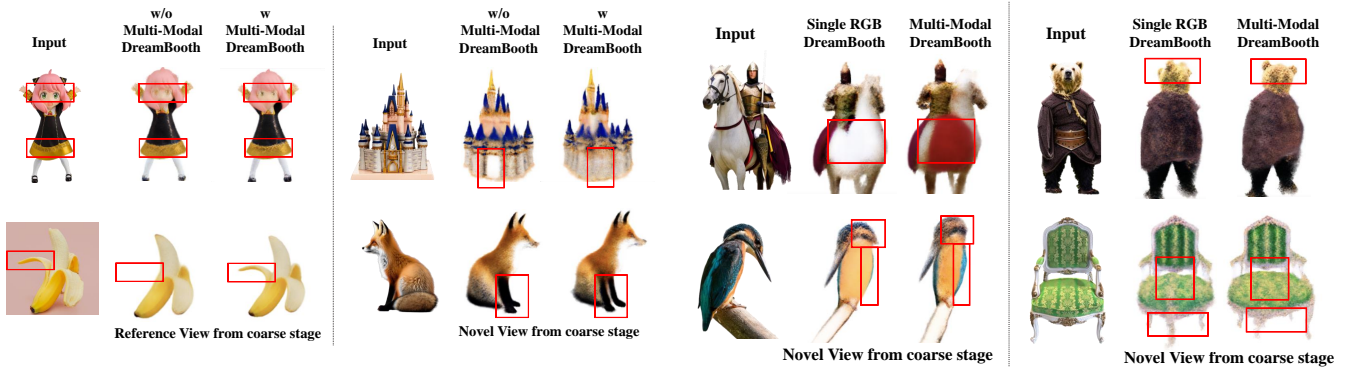


Figure 8. The effect of Multi-modal DreamBooth, showing a consistent improvement in terms of both geometry and texture.

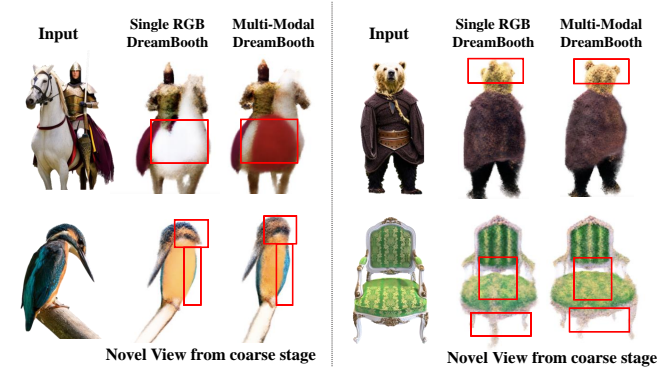


Figure 9. Single RGB versus Multi-modal DreamBooth, showing a clear improvement particularly in geometry.

Figure 11 presents several visual examples, verifying the efficacy of our method in modeling real scenes with a high degree of capability and fidelity.

7. Conclusion

We have presented Customize-It-3D, a novel two-stage approach for image-to-3D generation. Leveraging the estab-

lished customized knowledge prior, we enhances NeRF optimization for improved geometry and refines texture, resulting in superior alignment of 3D content with the subject. Customize-It-3D demonstrates versatility in handling general objects and empowers captivating applications.



Figure 10. Illustrating high-fidelity text-to-3D generation.

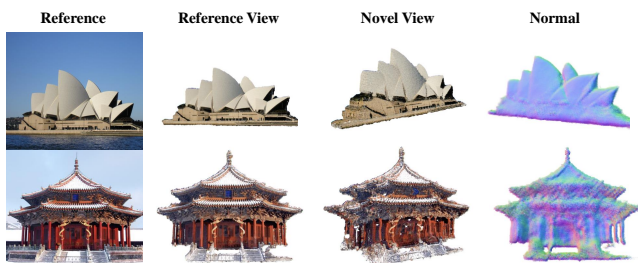


Figure 11. Illustrating high-fidelity 3D creation for real scenes.

References

- [1] Sameer Agarwal, Yasutaka Furukawa, Noah Snavely, Ian Simon, Brian Curless, Steven M Seitz, and Richard Szeliski. Building rome in a day. *Communications of the ACM*, 54(10):105–112, 2011. [2](#)
- [2] Titas Anciukevičius, Zexiang Xu, Matthew Fisher, Paul Henderson, Hakan Bilen, Niloy J Mitra, and Paul Guerrero. Renderdiffusion: Image diffusion for 3d reconstruction, inpainting and generation. In *Proceedings of the IEEE/CVF Conference on Computer Vision and Pattern Recognition*, pages 12608–12618, 2023. [3](#)
- [3] Yogesh Balaji, Seungjun Nah, Xun Huang, Arash Vahdat, Jiaming Song, Karsten Kreis, Miika Aittala, Timo Aila, Samuli Laine, Bryan Catanzaro, et al. ediffi: Text-to-image diffusion models with an ensemble of expert denoisers. *arXiv preprint arXiv:2211.01324*, 2022. [2](#)
- [4] Eric R Chan, Koki Nagano, Matthew A Chan, Alexander W Bergman, Jeong Joon Park, Axel Levy, Miika Aittala, Shalini De Mello, Tero Karras, and Gordon Wetzstein. Genvs: Generative novel view synthesis with 3d-aware diffusion models, 2023. [3](#)
- [5] Anpei Chen, Zexiang Xu, Andreas Geiger, Jingyi Yu, and Hao Su. Tensorf: Tensorial radiance fields. In *European Conference on Computer Vision*, pages 333–350. Springer, 2022. [2](#)
- [6] Anpei Chen, Zexiang Xu, Xinyue Wei, Siyu Tang, Hao Su, and Andreas Geiger. Dictionary fields: Learning a neural basis decomposition. *ACM Transactions on Graphics (TOG)*, 42(4):1–12, 2023. [2](#)
- [7] Hansheng Chen, Jiatao Gu, Anpei Chen, Wei Tian, Zhuowen Tu, Lingjie Liu, and Hao Su. Single-stage diffusion nerf: A unified approach to 3d generation and reconstruction. *arXiv preprint arXiv:2304.06714*, 2023. [3](#)
- [8] Rui Chen, Yongwei Chen, Ningxin Jiao, and Kui Jia. Fantasia3d: Disentangling geometry and appearance for high-quality text-to-3d content creation. *arXiv preprint arXiv:2303.13873*, 2023. [3](#)
- [9] Yen-Chi Cheng, Hsin-Ying Lee, Sergey Tulyakov, Alexander G Schwing, and Liang-Yan Gui. Sdfusion: Multimodal 3d shape completion, reconstruction, and generation. In *Proceedings of the IEEE/CVF Conference on Computer Vision and Pattern Recognition*, pages 4456–4465, 2023. [3](#)
- [10] Matt Deitke, Ruoshi Liu, Matthew Wallingford, Huong Ngo, Oscar Michel, Aditya Kusupati, Alan Fan, Christian Laforte, Vikram Voleti, Samir Yitzhak Gadre, Eli VanderBilt, Aniruddha Kembhavi, Carl Vondrick, Georgia Gkioxari, Kiana Ehsani, Ludwig Schmidt, and Ali Farhadi. Objaverse-xl: A universe of 10m+ 3d objects. *arXiv preprint arXiv:2307.05663*, 2023. [4](#)
- [11] Yilun Du, Cameron Smith, Ayush Tewari, and Vincent Sitzmann. Learning to render novel views from wide-baseline stereo pairs. In *Proceedings of the IEEE/CVF Conference on Computer Vision and Pattern Recognition*, pages 4970–4980, 2023. [2](#)
- [12] Ainaz Eftekhari, Alexander Sax, Jitendra Malik, and Amir Zamir. Omnidata: A scalable pipeline for making multi-task mid-level vision datasets from 3d scans. In *Proceedings of the IEEE/CVF International Conference on Computer Vision*, pages 10786–10796, 2021. [3](#)
- [13] Ziya Erkoç, Fangchang Ma, Qi Shan, Matthias Nießner, and Angela Dai. Hyperdiffusion: Generating implicit neural fields with weight-space diffusion. *arXiv preprint arXiv:2303.17015*, 2023. [3](#)
- [14] Yasutaka Furukawa, Carlos Hernández, et al. Multi-view stereo: A tutorial. *Foundations and Trends® in Computer Graphics and Vision*, 9(1-2):1–148, 2015. [2](#)
- [15] Jun Gao, Tianchang Shen, Zian Wang, Wenzheng Chen, Kangxue Yin, Daiqing Li, Or Litany, Zan Gojcic, and Sanja Fidler. Get3d: A generative model of high quality 3d textured shapes learned from images. *Advances In Neural Information Processing Systems*, 35:31841–31854, 2022. [3](#)
- [16] Jiatao Gu, Alex Trevithick, Kai-En Lin, Joshua M Susskind, Christian Theobalt, Lingjie Liu, and Ravi Ramamoorthi. Nerfdiff: Single-image view synthesis with nerf-guided distillation from 3d-aware diffusion. In *International Conference on Machine Learning*, pages 11808–11826. PMLR, 2023. [3](#)
- [17] Anchit Gupta, Wenhan Xiong, Yixin Nie, Ian Jones, and Barlas Ögüz. 3dgen: Triplane latent diffusion for textured mesh generation. *arXiv preprint arXiv:2303.05371*, 2023. [3](#)
- [18] Thomas A Halgren, Robert B Murphy, Richard A Friesner, Hege S Beard, Leah L Frye, W Thomas Pollard, and Jay L Banks. Glide: a new approach for rapid, accurate docking and scoring. 2. enrichment factors in database screening. *Journal of medicinal chemistry*, 47(7):1750–1759, 2004. [2](#)
- [19] Yukun Huang, Jianan Wang, Yukai Shi, Xianbiao Qi, Zheng-Jun Zha, and Lei Zhang. Dreamtime: An improved optimization strategy for text-to-3d content creation. *arXiv preprint arXiv:2306.12422*, 2023. [3](#)
- [20] Ajay Jain, Matthew Tancik, and Pieter Abbeel. Putting nerf on a diet: Semantically consistent few-shot view synthesis.

- In *Proceedings of the IEEE/CVF International Conference on Computer Vision*, pages 5885–5894, 2021. [2](#)
- [21] Ajay Jain, Ben Mildenhall, Jonathan T Barron, Pieter Abbeel, and Ben Poole. Zero-shot text-guided object generation with dream fields. In *Proceedings of the IEEE/CVF Conference on Computer Vision and Pattern Recognition*, pages 867–876, 2022. [3](#)
- [22] Heewoo Jun and Alex Nichol. Shap-e: Generating conditional 3d implicit functions. *arXiv preprint arXiv:2305.02463*, 2023. [3](#)
- [23] Oğuzhan Fatih Kar, Teresa Yeo, Andrei Atanov, and Amir Zamir. 3d common corruptions and data augmentation. In *Proceedings of the IEEE/CVF Conference on Computer Vision and Pattern Recognition*, pages 18963–18974, 2022. [3](#)
- [24] Animesh Karnawar, Niloy J Mitra, Andrea Vedaldi, and David Novotny. Holofusion: Towards photo-realistic 3d generative modeling. In *Proceedings of the IEEE/CVF International Conference on Computer Vision*, pages 22976–22985, 2023. [3](#)
- [25] Mijeong Kim, Seonguk Seo, and Bohyung Han. Infonerf: Ray entropy minimization for few-shot neural volume rendering. In *Proceedings of the IEEE/CVF Conference on Computer Vision and Pattern Recognition*, pages 12912–12921, 2022. [2](#)
- [26] Seung Wook Kim, Bradley Brown, Kangxue Yin, Karsten Kreis, Katja Schwarz, Daiqing Li, Robin Rombach, Antonio Torralba, and Sanja Fidler. Neuralfield-ldm: Scene generation with hierarchical latent diffusion models. In *Proceedings of the IEEE/CVF Conference on Computer Vision and Pattern Recognition*, pages 8496–8506, 2023. [3](#)
- [27] Alexander Kirillov, Eric Mintun, Nikhila Ravi, Hanzi Mao, Chloe Rolland, Laura Gustafson, Tete Xiao, Spencer Whitehead, Alexander C. Berg, Wan-Yen Lo, Piotr Dollár, and Ross Girshick. Segment anything. *arXiv:2304.02643*, 2023. [6](#)
- [28] Peter Kotschieder and Matthias Nießner. Diffrrf: Rendering-guided 3d radiance field diffusion-supplementary document. [3](#)
- [29] Nupur Kumari, Bingliang Zhang, Richard Zhang, Eli Shechtman, and Jun-Yan Zhu. Multi-concept customization of text-to-image diffusion. In *Proceedings of the IEEE/CVF Conference on Computer Vision and Pattern Recognition*, pages 1931–1941, 2023. [2](#)
- [30] Han-Hung Lee and Angel X Chang. Understanding pure clip guidance for voxel grid nerf models. *arXiv preprint arXiv:2209.15172*, 2022. [3](#)
- [31] Junnan Li, Dongxu Li, Silvio Savarese, and Steven C. H. Hoi. Blip-2: Bootstrapping language-image pre-training with frozen image encoders and large language models. *ArXiv*, abs/2301.12597, 2023. [5](#)
- [32] Chen-Hsuan Lin, Jun Gao, Luming Tang, Towaki Takikawa, Xiao-hui Zeng, Xun Huang, Karsten Kreis, Sanja Fidler, Ming-Yu Liu, and Tsung-Yi Lin. Magic3d: High-resolution text-to-3d content creation. In *IEEE Conference on Computer Vision and Pattern Recognition (CVPR)*, 2023. [3](#), [5](#)
- [33] Minghua Liu, Chao Xu, Haian Jin, Linghao Chen, Zexiang Xu, Hao Su, et al. One-2-3-45: Any single image to 3d mesh in 45 seconds without per-shape optimization. *arXiv preprint arXiv:2306.16928*, 2023. [3](#)
- [34] Ruoshi Liu, Rundi Wu, Basile Van Hoorick, Pavel Tokmakov, Sergey Zakharov, and Carl Vondrick. Zero-1-to-3: Zero-shot one image to 3d object, 2023. [3](#), [4](#), [7](#), [2](#)
- [35] Zhen Liu, Yao Feng, Michael J Black, Derek Nowrouzezahrai, Liam Paull, and Weiyang Liu. Meshdiffusion: Score-based generative 3d mesh modeling. *arXiv preprint arXiv:2303.08133*, 2023. [3](#)
- [36] Stephen Lombardi, Tomas Simon, Jason Saragih, Gabriel Schwartz, Andreas Lehrmann, and Yaser Sheikh. Neural volumes: Learning dynamic renderable volumes from images. *arXiv preprint arXiv:1906.07751*, 2019. [2](#)
- [37] Shitong Luo and Wei Hu. Diffusion probabilistic models for 3d point cloud generation. In *Proceedings of the IEEE/CVF Conference on Computer Vision and Pattern Recognition*, pages 2837–2845, 2021. [3](#)
- [38] Luke Melas-Kyriazi, Iro Laina, Christian Rupprecht, and Andrea Vedaldi. Realfusion: 360deg reconstruction of any object from a single image. In *Proceedings of the IEEE/CVF Conference on Computer Vision and Pattern Recognition*, pages 8446–8455, 2023. [1](#), [2](#), [3](#), [7](#), [8](#)
- [39] Ben Mildenhall, Pratul P. Srinivasan, Matthew Tancik, Jonathan T. Barron, Ravi Ramamoorthi, and Ren Ng. Nerf: Representing scenes as neural radiance fields for view synthesis. In *ECCV*, 2020. [2](#), [4](#)
- [40] Nasir Mohammad Khalid, Tianhao Xie, Eugene Belilovsky, and Tiberiu Popa. Clip-mesh: Generating textured meshes from text using pretrained image-text models. In *SIGGRAPH Asia 2022 conference papers*, pages 1–8, 2022. [3](#)
- [41] Thomas Müller, Alex Evans, Christoph Schied, and Alexander Keller. Instant neural graphics primitives with a multiresolution hash encoding. *ACM Trans. Graph.*, 41(4):102:1–102:15, 2022. [2](#), [4](#), [7](#)
- [42] Alex Nichol, Heewoo Jun, Prafulla Dhariwal, Pamela Mishkin, and Mark Chen. Point-e: A system for generating 3d point clouds from complex prompts. *arXiv preprint arXiv:2212.08751*, 2022. [3](#)
- [43] Evangelos Ntavelis, Aliaksandr Siarohin, Kyle Olszewski, Chaoyang Wang, Luc Van Gool, and Sergey Tulyakov. Autodecoding latent 3d diffusion models. *arXiv preprint arXiv:2307.05445*, 2023. [3](#)
- [44] Dustin Podell, Zion English, Kyle Lacey, Andreas Blattmann, Tim Dockhorn, Jonas Müller, Joe Penna, and Robin Rombach. Sdxl: Improving latent diffusion models for high-resolution image synthesis, 2023. [7](#)
- [45] Ben Poole, Ajay Jain, Jonathan T. Barron, and Ben Mildenhall. Dreamfusion: Text-to-3d using 2d diffusion. *arXiv*, 2022. [1](#), [3](#), [5](#), [6](#), [7](#)
- [46] Guocheng Qian, Jinjie Mai, Abdullah Hamdi, Jian Ren, Aliaksandr Siarohin, Bing Li, Hsin-Ying Lee, Ivan Skokhodov, Peter Wonka, Sergey Tulyakov, and Bernard Ghanem. Magic123: One image to high-quality 3d object generation using both 2d and 3d diffusion priors. *arXiv preprint arXiv:2306.17843*, 2023. [1](#), [2](#), [3](#), [7](#), [8](#)
- [47] Alec Radford, Jong Wook Kim, Chris Hallacy, Aditya Ramesh, Gabriel Goh, Sandhini Agarwal, Girish Sastry,

- Amanda Aspell, Pamela Mishkin, Jack Clark, et al. Learning transferable visual models from natural language supervision. In *International conference on machine learning*, pages 8748–8763. PMLR, 2021. 7
- [48] Amit Raj, Srinivas Kaza, Ben Poole, Michael Niemeyer, Ben Mildenhall, Nataniel Ruiz, Shiran Zada, Kfir Aberman, Michael Rubenstein, Jonathan Barron, Yuanzhen Li, and Varun Jampani. Dreambooth3d: Subject-driven text-to-3d generation. *ICCV*, 2023. 3
- [49] Aditya Ramesh, Prafulla Dhariwal, Alex Nichol, Casey Chu, and Mark Chen. Hierarchical text-conditional image generation with clip latents. *arXiv preprint arXiv:2204.06125*, 1(2):3, 2022. 2
- [50] René Ranftl, Katrin Lasinger, David Hafner, Konrad Schindler, and Vladlen Koltun. Towards robust monocular depth estimation: Mixing datasets for zero-shot cross-dataset transfer. *IEEE Transactions on Pattern Analysis and Machine Intelligence*, 44(3), 2022. 3, 5
- [51] Robin Rombach, Andreas Blattmann, Dominik Lorenz, Patrick Esser, and Björn Ommer. High-resolution image synthesis with latent diffusion models, 2021. 2, 3, 4, 1
- [52] Nataniel Ruiz, Yuanzhen Li, Varun Jampani, Yael Pritch, Michael Rubenstein, and Kfir Aberman. Dreambooth: Fine tuning text-to-image diffusion models for subject-driven generation. In *Proceedings of the IEEE/CVF Conference on Computer Vision and Pattern Recognition*, 2023. 2, 3
- [53] Chitwan Saharia, William Chan, Saurabh Saxena, Lala Li, Jay Whang, Emily L Denton, Kamyar Ghasemipour, Raphael Gontijo Lopes, Burcu Karagol Ayan, Tim Salimans, et al. Photorealistic text-to-image diffusion models with deep language understanding. *Advances in Neural Information Processing Systems*, 35:36479–36494, 2022. 2
- [54] Johannes L Schonberger and Jan-Michael Frahm. Structure-from-motion revisited. In *Proceedings of the IEEE conference on computer vision and pattern recognition*, pages 4104–4113, 2016. 2
- [55] Johannes L Schönberger, Enliang Zheng, Jan-Michael Frahm, and Marc Pollefeys. Pixelwise view selection for unstructured multi-view stereo. In *Computer Vision—ECCV 2016: 14th European Conference, Amsterdam, The Netherlands, October 11–14, 2016, Proceedings, Part III 14*, pages 501–518. Springer, 2016. 2
- [56] Hoigi Seo, Hayeon Kim, Gwanghyun Kim, and Se Young Chun. Ditto-nerf: Diffusion-based iterative text to omnidirectional 3d model. *arXiv preprint arXiv:2304.02827*, 2023. 3
- [57] Yichun Shi, Peng Wang, Jialong Ye, Mai Long, Kejie Li, and Xiao Yang. Mvdream: Multi-view diffusion for 3d generation. *arXiv preprint arXiv:2308.16512*, 2023. 3
- [58] Jingxiang Sun, Bo Zhang, Ruizhi Shao, Lizhen Wang, Wen Liu, Zhenda Xie, and Yebin Liu. Dreamcraft3d: Hierarchical 3d generation with bootstrapped diffusion prior. *arXiv preprint arXiv:2310.16818*, 2023. 1
- [59] Stanislaw Szymanowicz, Christian Rupprecht, and Andrea Vedaldi. Viewset diffusion:(0-) image-conditioned 3d generative models from 2d data. *arXiv preprint arXiv:2306.07881*, 2023. 3
- [60] Junshu Tang, Tengfei Wang, Bo Zhang, Ting Zhang, Ran Yi, Lizhuang Ma, and Dong Chen. Make-it-3d: High-fidelity 3d creation from a single image with diffusion prior. In *Proceedings of the IEEE/CVF International Conference on Computer Vision (ICCV)*, pages 22819–22829, 2023. 1, 2, 3, 5, 6, 7, 8
- [61] Christina Tsalicoglou, Fabian Manhardt, Alessio Tonioni, Michael Niemeyer, and Federico Tombari. Textmesh: Generation of realistic 3d meshes from text prompts. *arXiv preprint arXiv:2304.12439*, 2023. 3
- [62] Patrick von Platen, Suraj Patil, Anton Lozhkov, Pedro Cuenca, Nathan Lambert, Kashif Rasul, Mishig Davaadorj, and Thomas Wolf. Diffusers: State-of-the-art diffusion models. <https://github.com/huggingface/diffusers>, 2022. 4
- [63] Haochen Wang, Xiaodan Du, Jiahao Li, Raymond A Yeh, and Greg Shakhnarovich. Score jacobian chaining: Lifting pretrained 2d diffusion models for 3d generation. In *Proceedings of the IEEE/CVF Conference on Computer Vision and Pattern Recognition*, pages 12619–12629, 2023. 3
- [64] Tengfei Wang, Bo Zhang, Ting Zhang, Shuyang Gu, Jianmin Bao, Tadas Baltrusaitis, Jingjing Shen, Dong Chen, Fang Wen, Qifeng Chen, et al. Rodin: A generative model for sculpting 3d digital avatars using diffusion. In *Proceedings of the IEEE/CVF Conference on Computer Vision and Pattern Recognition*, pages 4563–4573, 2023. 3
- [65] Zhengyi Wang, Cheng Lu, Yikai Wang, Fan Bao, Chongxuan Li, Hang Su, and Jun Zhu. Prolificdreamer: High-fidelity and diverse text-to-3d generation with variational score distillation. *arXiv preprint arXiv:2305.16213*, 2023. 1, 3
- [66] Daniel Watson, William Chan, Ricardo Martin-Brualla, Jonathan Ho, Andrea Tagliasacchi, and Mohammad Norouzi. Novel view synthesis with diffusion models. *arXiv preprint arXiv:2210.04628*, 2022. 3
- [67] Jiaxin Xie, Hao Ouyang, Jingtian Piao, Chenyang Lei, and Qifeng Chen. High-fidelity 3d gan inversion by pseudo-multi-view optimization. *arXiv preprint arXiv:2211.15662*, 2022. 6
- [68] Xingyu Xie, Pan Zhou, Huan Li, Zhouchen Lin, and Shuicheng Yan. Adan: Adaptive nesterov momentum algorithm for faster optimizing deep models. *arXiv preprint arXiv:2208.06677*, 2022. 1
- [69] Dejia Xu, Yifan Jiang, Peihao Wang, Zhiwen Fan, Yi Wang, and Zhangyang Wang. Neuralift-360: Lifting an in-the-wild 2d photo to a 3d object with 360deg views. In *Proceedings of the IEEE/CVF Conference on Computer Vision and Pattern Recognition*, pages 4479–4489, 2023. 1
- [70] Lior Yariv, Yoni Kasten, Dror Moran, Meirav Galun, Matan Atzmon, Basri Ronen, and Yaron Lipman. Multiview neural surface reconstruction by disentangling geometry and appearance. *Advances in Neural Information Processing Systems*, 33, 2020. 5
- [71] Alex Yu, Vickie Ye, Matthew Tancik, and Angjoo Kanazawa. pixelnerf: Neural radiance fields from one or few images. In *Proceedings of the IEEE/CVF Conference on Computer Vision and Pattern Recognition*, pages 4578–4587, 2021. 2
- [72] Jiahui Yu, Zhe Lin, Jimei Yang, Xiaohui Shen, Xin Lu, and

- Thomas S Huang. Free-form image inpainting with gated convolution. *arXiv preprint arXiv:1806.03589*, 2018. 7, 1
- [73] Xiaohui Zeng, Arash Vahdat, Francis Williams, Zan Gojcic, Or Litany, Sanja Fidler, and Karsten Kreis. Lion: Latent point diffusion models for 3d shape generation. *arXiv preprint arXiv:2210.06978*, 2022. 3
- [74] Biao Zhang, Jiapeng Tang, Matthias Niessner, and Peter Wonka. 3dshape2vecset: A 3d shape representation for neural fields and generative diffusion models. *arXiv preprint arXiv:2301.11445*, 2023. 3
- [75] Richard Zhang, Phillip Isola, Alexei A Efros, Eli Shechtman, and Oliver Wang. The unreasonable effectiveness of deep features as a perceptual metric. In *Proceedings of the IEEE conference on computer vision and pattern recognition*, pages 586–595, 2018. 7
- [76] Linqi Zhou, Yilun Du, and Jiajun Wu. 3d shape generation and completion through point-voxel diffusion. In *Proceedings of the IEEE/CVF International Conference on Computer Vision*, pages 5826–5835, 2021. 3

Customize-It-3D: High-Quality 3D Creation from A Single Image Using Subject-Specific Knowledge Prior

Supplementary Material

A. Additional Implementation Details

A.1. Coarse stage

Multi-modal Dreambooth finetuning and usage. We utilized the stable diffusion V2.0 model [51] in our experiments. We employed multi-modal images related to the reference image and conducted a four-step fine-tuning process on the diffusion model. The sequence and number of iterations for each training step are as follows: 25 iterations for mask image training, 50 iterations for depth image training, 50 iterations for normal image training, and 75 iterations for RGB image training, totaling 200 iterations. During fine-tuning, prompts were specified as follows: “a foreground mask / depth map / normal map / RGB photo of sks [class_name].” When using the finetuned model for training in the coarse stage, we modified the prompts based on shading mode. For normal shading, we append the modifier “normal map” to the text prompt, while for other shading strategies, we add the modifier “RGB photo”. We observed that this approach facilitated the better utilization of subject-specific knowledge, leading to improved results.

Optimizing the pipeline. We employ the Adam optimizer [68] with a learning rate of 0.005 and no weight decay for 7000 iterations. Simultaneously, during the coarse stage, we implement progressive training, where the first 2000 iterations exclusively trained within the range of $\pm 45^\circ$ from the reference view, and the subsequent 5000 iterations covered the entire 360° around the object. In the refine stage, we conducted 3000 iterations to optimize the texture.

Camera setting. For the camera sampling method, we randomly sample novel views with a probability of 75%, while with a 25% probability, we sample a reference view following the approach in [45]. The reference view is assumed to be a frontal view, i.e., a polar angle of 90° and an azimuth angle of 0° . It is further assumed that the camera is positioned at a distance of 1 meter from the origin of the coordinate system, and the field of view (FOV) is set to 60° .

A.2. Refine stage

Post-mask processing. We also perform post-mask-processing, wherein we apply certain morphological operations to both SAM-generated and NeRF-generated masks, i.e., taking the union of the two masks to complement fine structures lacking in the initial mask. Finally, we have $M_{pseudo} = \hat{M} \cup \hat{M}_{SAM}$, where \hat{M} and \hat{M}_{sam} are the rendering and SAM-generated mask after post-processing under novel view.

Point cloud building. The goal of our point cloud building strategy is to avoid introducing points with color conflicts that overlap with existing point cloud p_{ref}^m , which is build from reference view. We use a reference mask M_{pseudo}^{ref} to perform color mapping on p_{ref}^m , obtaining the front-facing perspective of the new point cloud p_{ref} . For all remaining regions under novel view, we project the just obtained point cloud p_{ref} onto each novel view v_i to create a new mask m_i^{re} . We then take the set difference between the novel view mask m_{pseudo}^i and the re-projected mask m_i^{re} as the mask for the remaining points $P_{left} = P^m - p_{ref}^m$. Finally we will have a clean point cloud $P = \{p_{ref}, p_1, \dots, p_n\}$ which ensures color mapping is done without introducing conflicts.

Point cloud rendering. In order to perform better point cloud rendering, each point’s has a 19-dimensional descriptor, with the initial three dimensions initialized with RGB colors and the rest initialized randomly [60]. Deferred rendering is conducted for a total of $K = 3$ times, with resolutions denoted as $[H/2^i, W/2^i]$, where $i \in [0, K)$ and ultimately, the learned U-Net network concatenates these three feature maps. And the U-Net architecture contains 3 down-sampling and up-sampling layers with gated convolutions[72]. The rendering resolution is set to 128×128 in the coarse stage for NeRF and 800×800 in the refine stage for the point cloud, respectively.

B. Additional Ablation Study Results

As mentioned in the paper, current methods for text/image-to-3D rely on a generic diffusion model with strong generalization capabilities, leveraging implicit 2D knowledge to guide the generation of novel views. However, due to its overly rich imagination, this model may generate 3D objects that do not align with the subject identity. To address this limitation, we fine-tune the diffusion model to learn subject-oriented knowledge. We conduct a series of experiments to demonstrate the effectiveness of our subject-specific and multi-modal diffusion model. We first ablate the effect of using the proposed multi-modal Dreambooth, as illustrated in Figure 13. The results indicate that without the guidance of our multi-modal Dreambooth, the coarse stage produces textures and geometry that deviate from the subject identity, thereby impacting the initialization of point cloud geometry and textures in the refine stage, as exemplified by the patterns on the fox’s neck and the rabbit’s ears.

Furthermore, we compare the results obtained using the traditional dreambooth (trained with a single RGB image)



Figure 12. Additional comparison with baseline: RealFusion [38], Make-It-3D [60], and Magic123 [46]. The first column is the reference image.

	LPIPS↓	PSNR↑	CLIP↑
RealFusion [38]	0.197	16.41	70.08%
Make-It-3D [60]	0.121	19.31	78.93%
Magic123 [46]	0.098	20.10	85.70%
Customize-It-3D (Ours)	0.096	20.30	91.08%

Table 2. Quantitative comparison on our dataset. We compute LPIPS, PSNR and CLIP-similarity.

with our multi-modal dreambooth (trained with multiple multi-modal images). We also compare the results of the NeRF training process with and without shading mode guidance. Both sets of experiments are depicted in Figure 14. The results show that a simple attempt using only dreambooth leads to overfitting and mode collapse. Additionally, we observed that using shading mode guidance better leverages our multi-modal dreambooth, resulting in more convergent and 3D-consistent outcomes.

C. Additional Comparisons with Baseline

In this section, we show more results comparing our method with the baseline: RealFusion [38], Make-It-3D [60], and Magic123 [46] (using Zero123 XL checkpoint [34]), as shown in the Figure 12. Also we do quantitative comparison on our own dataset as shown in the Table 2, and our method has the best results. Results show that our method exhibits increased fidelity to the input reference image in both geometry and texture, thanks to the utilization of subject-specific knowledge priors. This incorporation makes the training process more aligned with the subject’s identity. Particularly in terms of texture, as exemplified in the second row with the silver cat in the Figure 12, our method generates back textures with a more pronounced metallic sheen, consistent with the characteristics of the front texture. Similarly, as seen in the fifth row with the doll in the Figure 12, our method generates doll textures on the back and sides, including patterns on the skirt and hair color, that better align

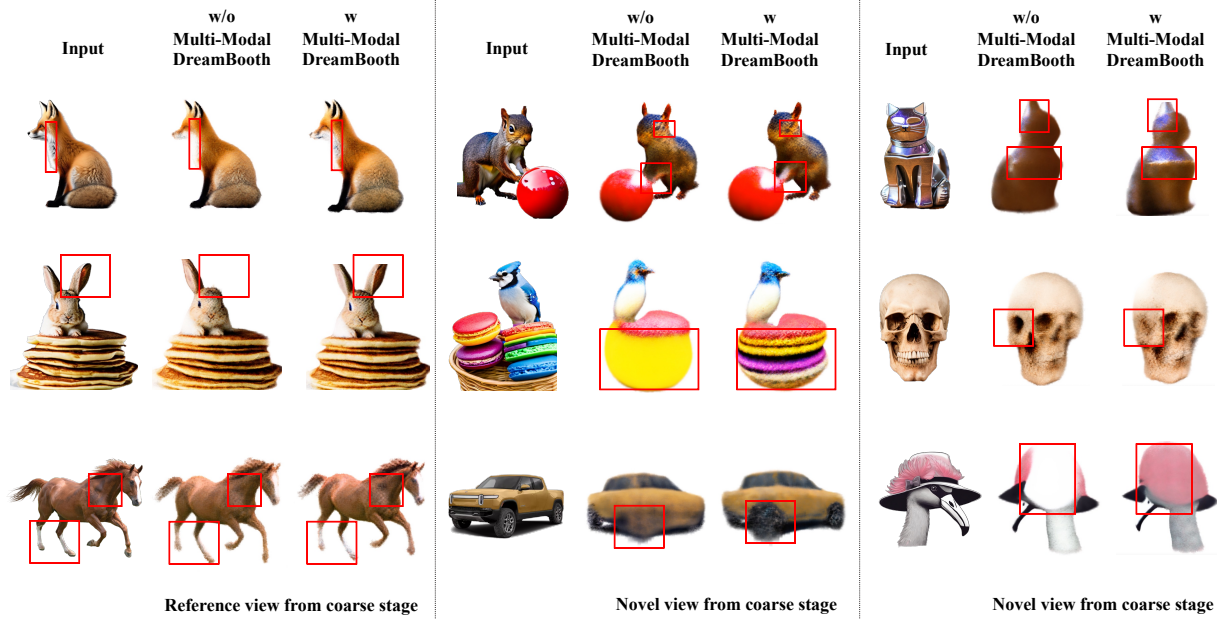


Figure 13. Additional results of an ablation study on whether to use the multi-modal dreambooth. The first column is the reference image.

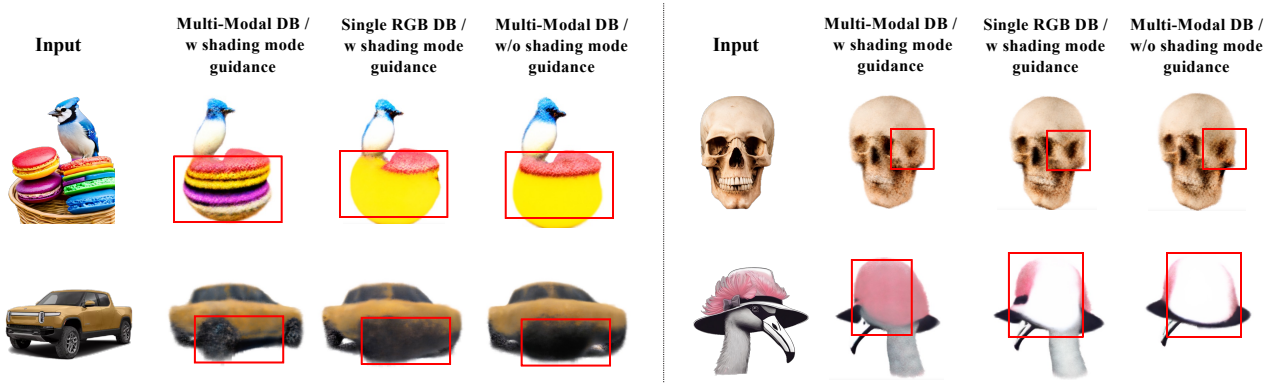


Figure 14. Additional ablation results. The first column is the reference image. The second column displays the results obtained using our method. The third column showcases the outcomes when substituting the multi-modal dreambooth with the traditional dreambooth. The fourth column exhibits the results when shading mode guidance is omitted during the NeRF training process.

with the subject’s identity. Therefore, our method is capable of generating textures that are more consistent with the reference view.

D. Additional Results

In this section, we show more results using our method. Figure 15 and Figure 16 demonstrates the ability of our method to generate high-quality 3D objects from a single image.

E. Limitation

Our method has several limitations. Firstly, because our approach relies on using pretrained models as depth esti-

mator [50] and normal estimator [12] [23] to estimate the depth map and normal map of the reference image. So any errors in these modules will affect our method and impact the overall generation quality. Also, our method, relying on generative prior to imagine the 3D content from the single reference viewpoint, inevitably introduces geometry ambiguity [45], leading to issues such as the Janus problem or over-flat geometry.



Figure 15. Additional results by *Customize-It-3D*. The first column is the reference image.



Figure 16. Additional results by *Customize-It-3D*. The first column is the reference image.